RESEARCH PAPER

Formulation Optimisation of Cilnidipine-Loaded Solid Lipid Nanoparticles Using Box-Behnken Statistical Design: Physicochemical Characterisation and In Vitro Drug Release Evaluation

Nishant Yadav[1], Parveen Kumar[2], Teenu Sharma[1], Sushma Devi[1*]

[1]Chitkara College of Pharmacy, Chitkara University, Rajpura, Punjab
[2]Nims Institute of Pharmacy, Nims University Rajasthan, Jaipur
[*]Corresponding Author: sushma.mehla@gmail.com

ABSTRACT

Cilnidipine, a calcium channel blocker indicated for the management of hypertension, exhibits poor aqueous solubility and low oral bioavailability, thereby limiting its therapeutic effectiveness. This study formulated, statistically optimised, and characterised cilnidipine-loaded solid lipid nanoparticles (SLNs) using a Box-Behnken design with three factors at three levels (17 runs). Compritol 888 ATO (glycerol dibehenate), Poloxamer 188, and Tween 80 served as the lipid matrix, steric stabiliser, and co-surfactant, respectively. The effects of these variables on three critical quality attributes—particle size (PS), entrapment efficiency (EE), and polydispersity index (PDI)—were systematically assessed using response surface methodology (RSM). SLNs were prepared via melt-emulsification and high-shear homogenisation. The quadratic model was statistically significant for all three responses. Compritol concentration was the primary determinant for PS ($F = 272.12$, $p < 0.0001$) and PDI ($F = 36.84$, $p < 0.0005$), while a synergistic interaction between Compritol and Poloxamer 188 influenced EE ($F = 32.87$, $p < 0.001$). The optimised formulation (Compritol-10 g, Poloxamer 188-15 g, Tween 80-2.5 mL) yielded SLNs with a mean PS of 122 nm, a zeta potential of −41.05 mV, and an EE of 84.34%. Scanning electron microscopy (SEM) indicated spherical to oval particles with smooth surfaces. In vitro drug release in PBS (pH 7.4, 37°C) exhibited a biphasic profile: an initial burst release of approximately 30.68% within 1 hour, followed by sustained release reaching 83.46% at 24 hours. These results indicate that SLNs represent a promising colloidal carrier system for enhancing the controlled delivery of cilnidipine and may improve its transdermal application.

Keywords: Solid lipid nanoparticles; Cilnidipine; Box-Behnken design; Sustained release; Transdermal drug delivery

How to cite this article: Yadav N, Kumar P, Sharma T, Devi S. Formulation Optimisation of Cilnidipine-Loaded Solid Lipid Nanoparticles Using Box-Behnken Statistical Design: Physicochemical Characterisation and In Vitro Drug Release Evaluation. Int J Drug Deliv Technol. 2026;16(51s): 412-423. DOI: 10.25258/ijddt.16.51s.29

Source of support: Nil.
Conflict of interest: None

1. INTRODUCTION

Hypertension constitutes one of the most prevalent non-communicable diseases globally, affecting over 1.28 billion adults and representing a leading modifiable risk factor for cardiovascular morbidity and mortality [1]. Among antihypertensive agents, calcium channel blockers (CCBs) occupy a prominent therapeutic position owing to their potent vasodilatory activity and demonstrated cardiovascular protective effects [2,3]. Cilnidipine — a third-generation, dual N/L-type calcium channel blocker — offers a pharmacodynamically superior profile compared to conventional dihydropyridines such as amlodipine or nifedipine. Its simultaneous blockade of L-type and N-type calcium channels reduces peripheral vascular resistance and suppresses sympathetic neurotransmitter release, thereby mitigating reflex tachycardia — a recognised limitation of older CCBs [4].

Despite its favourable pharmacodynamic profile, cilnidipine presents significant biopharmaceutical challenges. As a BCS Class II compound, it exhibits poor aqueous solubility (~0.1 µg/mL), resulting in dissolution-rate-limited oral absorption and low, highly variable bioavailability (~13%) [5,6]. These limitations necessitate exploring advanced drug-delivery strategies to improve solubility, absorption, and therapeutic efficacy.

Solid lipid nanoparticles (SLNs) have emerged as a compelling colloidal carrier system for addressing the biopharmaceutical challenges of poorly water-soluble drugs [7,8]. SLNs offer a distinctive set of advantages: they are fabricated from biocompatible, biodegradable

lipid matrices; they protect chemically labile drugs from degradation; they enable controlled and sustained drug release through diffusion-mediated mechanisms; they enhance transdermal permeation owing to their nanoscale dimensions; and they can be engineered with precisely tunable physicochemical properties [9,10]. These attributes make SLNs particularly well-suited for both oral and transdermal delivery of lipophilic drugs such as cilnidipine.

Critical quality attributes (CQAs) of SLNs — including particle size, zeta potential, polydispersity index, and drug entrapment efficiency — are governed by complex, non-linear interactions among formulation variables: lipid concentration, surfactant identity and concentration, and co-surfactant levels. Classical one-variable-at-a-time (OVAT) optimisation approaches fail to capture these interactions and cannot identify a true multivariate optimum. Quality by Design (QbD) statistical methodologies — particularly Box-Behnken design (BBD) with response surface methodology (RSM) — offer a rigorous, systematic framework for simultaneously studying multiple variables, modelling their effects and interactions, and identifying optimal design spaces [11,12].

The present study therefore aimed to: (i) apply a Box-Behnken design to systematically optimise three critical formulation variables (Compritol 888 ATO, Poloxamer 188, and Tween 80) with respect to PS, EE, and PDI; (ii) prepare the optimised cilnidipine SLN formulation by melt-emulsification/high-shear homogenisation; (iii) comprehensively characterise the optimised formulation and (iv) evaluate in vitro drug release behavior to confirm suitability for sustained and potential transdermal delivery.

2. MATERIALS AND METHODS

2.1 Materials

Cilnidipine was obtained as a gift sample from Pure & Cure Healthcare Pvt. Ltd, Haridwar, India. Compritol 888 ATO (glycerol dibehenate) was sourced from Gettefosse (India) Pvt. Ltd; Mumbai. BASF, India, supplied Poloxamer 188 (Lutrol F68). Tween 80 (polysorbate 80) was procured from S. D. Fine Chem. Ltd., Mumbai. Isopropyl alcohol (IPA) and all other reagents and solvents were of analytical grade and used as received; an in-house Milli-Q purification system produced purified water.

2.2 Experimental Design — Box-Behnken Design

A Box-Behnken design (BBD), a three-factor three-level response surface design, was employed to systematically investigate the influence of formulation variables on the critical quality attributes (CQAs). The BBD requires 17 experimental runs (including 5 centre-point replicates) for three factors, enabling estimation of all linear, quadratic and two-factor interaction terms of the second-order polynomial model while avoiding vertex (corner) points that may represent extreme or impractical formulation conditions. The design matrix was generated using Design Expert® software v13.0. Independent variables (critical process parameters, CPPs) and their levels are listed in Table 1.

Table 1. Independent variables and their coded levels in the Box-Behnken design.

Code	Factor / Ingredient	Low (−1)	High (+1)	Unit
A	Compritol 888 ATO (Glycerol Dibehenate)	8.00	12.00	g
B	Poloxamer 188 (Lutrol F68)	10.00	20.00	g
C	Tween 80	1.00	4.00	mL

The dependent variables (responses) measured were: Y_1 — Particle Size (nm); Y_2 — Entrapment Efficiency (%); and Y_3 — Polydispersity Index (PDI). The quadratic polynomial model relating each response to the coded factors was:

$$Y = \beta_0 + \beta_1 A + \beta_2 B + \beta_3 C + \beta_{12} AB + \beta_{13} AC + \beta_{23} BC + \beta_{11} A^2 + \beta_{22} B^2 + \beta_{33} C^2$$

where Y is the predicted response, β_0 is the model intercept, β_1–β_3 are linear coefficients, β_{12}, β_{13}, β_{23} are two-factor interaction coefficients, and β_{11}, β_{22}, β_{33} are quadratic coefficients. Model selection was based on sequential p-value analysis, adjusted R^2, predicted R^2, and the PRESS statistic.

2.3 Preparation of Optimised Cilnidipine-Loaded SLNs

The optimised cilnidipine-loaded SLNs were prepared by melt-emulsification followed by high-shear homogenisation. The composition of the optimised formulation is shown in Table 2.

Table 2. Composition of the optimised cilnidipine-loaded SLN formulation.

Ingredient	Quantity
Cilnidipine (Drug)	100.0 mg
Compritol 888 ATO (Glycerol Dibehenate)	10.0 g
Tween 80	2.5 mL
Poloxamer 188 (Lutrol F68)	15.0 g
Purified Water	q.s.

Step 1 —Preparation of Aqueous Phase

A sufficient quantity of purified water was taken in a beaker and heated to 85–90°C on a magnetic hot plate stirrer. Poloxamer 188 and Tween 80 were added sequentially under continuous stirring until a clear, homogeneous aqueous solution was obtained.

Step 2 — Preparation of Lipid Phase

In a separate beaker, Compritol 888 ATO was heated above its melting point (~70°C) to achieve complete melting. Cilnidipine (100 mg), previously dissolved in the required quantity of isopropyl alcohol (IPA), was added to the molten lipid under constant magnetic stirring. The mixture was maintained at 85–90°C with continuous stirring until a clear, homogeneous lipid-drug solution was obtained, confirming complete drug incorporation into the molten matrix.

Step 3 — Emulsification and High-Shear Homogenization

The molten lipid phase (Step 2) was slowly poured into the preheated aqueous phase (Step 1), maintained at 85–90°C under continuous mechanical agitation. The resulting pre-emulsion was subjected to high-shear homogenisation at 14,000 rpm for 20 minutes using a high-speed homogeniser, while maintaining a temperature of 85–90°C, to generate a uniform hot nanoemulsion.

Step 4 — Solidification and SLN Formation

Following homogenisation, the hot nanoemulsion was allowed to cool to room temperature under gentle, continuous magnetic stirring. This cooling step facilitated simultaneous: (i) solidification of the dispersed lipid droplets to form the SLN core, and (ii) evaporation of the residual isopropyl alcohol used as the drug-dissolving solvent. The dispersion was stored at 4°C for further characterisation.

2.4 Physicochemical Characterisation

2.4.1 Particle Size, PDI, and Zeta Potential

Mean particle size, polydispersity index (PDI), and zeta potential of the optimised SLN dispersion were determined by dynamic light scattering (DLS) using a Malvern Zetasizer Nano ZS at 25°C [13]. All analyses were performed in triplicate (n = 3).

2.4.2 Percent Entrapment Efficiency

Entrapment efficiency (EE%) was determined by an indirect method [14,15]. A weighed quantity of the SLN dispersion was diluted with methanol to disrupt the nanoparticle structure and release the entrapped drug. The mixture was centrifuged at 8,000 rpm for 10 minutes; the supernatant containing the free (unentrapped) drug fraction was collected, and drug concentration was quantified by UV spectrophotometry at 240 nm using a validated calibration curve. EE% was calculated as:

$$\text{EE (\%)} = [(\text{Total Drug Added} - \text{Free Drug in Supernatant}) / \text{Total Drug Added}] \times 100$$

2.4.3 Morphological Assessment by Scanning Electron Microscopy

Surface morphology of the optimised SLNs was examined by scanning electron microscopy (SEM) [16]. Images were captured at appropriate magnifications.2.5 In Vitro Drug Release Studies

2.5. In Vitro Drug Release Study

In vitro drug release from the optimised cilnidipine SLNs was evaluated using the dialysis membrane diffusion method [17,18]. The dialysis membrane was soaked in purified water for 12 hours before use. A quantity of SLN dispersion equivalent to 5 mg of cilnidipine was sealed in the dialysis bag. The bag was then suspended in 250 mL of phosphate-buffered saline (PBS, pH 7.4) containing 1% w/v Tween 80 as the release medium, maintained at 37 ± 0.5°C with constant magnetic stirring at 75 rpm to simulate physiological plasma conditions.

Aliquots of 1 mL were withdrawn at predetermined time intervals (0, 0.25, 0.5, 0.75, 1, 2, 4, 6, 8, 10, 12, and 24 h) and replaced immediately with an equal volume of fresh, preheated dissolution medium to maintain sink conditions. Withdrawn samples were analysed spectrophotometrically at 240 nm. Cumulative per cent drug release (CDR%) was calculated at each time point. The experiment was conducted in triplicate (n = 3), and results are expressed as mean ± standard deviation (SD).

2.6 Statistical Analysis

All statistical analyses were performed using Design Expert v13.0 software. ANOVA was applied to evaluate the significance of the model and individual factor effects. Diagnostic adequacy was assessed using residual plots, predicted-versus-actual plots, Cook's distance, and leverage values. Results are reported as mean ± SD; $p < 0.05$ was considered statistically significant.

3. RESULTS AND DISCUSSION

3.1 Box-Behnken Design — Experimental Matrix

The complete BBD experimental matrix comprising 17 runs, along with the observed responses for PS (Y_1), EE (Y_2), and PDI (Y_3), is presented in Table 3. Particle size ranged from 100.00 nm (Run 8; lowest Compritol) to 125.00 nm (Run 12; highest Compritol, lowest Poloxamer), with a mean of 110.37 nm — demonstrating that all 17 formulations consistently achieved sub-150 nm particle dimensions. EE ranged from 78.00% (Run 8) to 97.00% (Run 4; high Compritol and Poloxamer), with a mean of 86.00%. PDI ranged from 0.450 (Run 8) to 0.891 (Run 12), indicating a broad formulation space from moderately monodisperse to highly polydisperse systems.

Table 3. Box-Behnken design matrix with observed responses (Y_1: PS, Y_2: EE, Y_3: PDI; n = 3).

Std	Run	A: Compritol (g)	B: Poloxamer 188 (g)	C: Tween 80 (mL)	Y_1: PS (nm)	Y_2: EE (%)	Y_3: PDI
8	1	12	15	4	121.00	91	0.670
7	2	8	15	4	104.00	82	0.489
1	3	8	10	2.5	103.54	88	0.541
4	4	12	20	2.5	120.00	97	0.874
3	5	8	20	2.5	104.00	82	0.589
9	6	10	10	1	110.00	88	0.690
10	7	10	20	1	107.00	89	0.650
5	8	8	15	1	100.00	78	0.450
6	9	12	15	1	115.00	89	0.684
15	10	10	15	2.5	109.84	81	0.700
12	11	10	20	4	110.00	92	0.723
2	12	12	10	2.5	125.00	85	0.891
16	13	10	15	2.5	109.85	84	0.780
17	14	10	15	2.5	110.00	83	0.712
14	15	10	15	2.5	108.00	84	0.622
13	16	10	15	2.5	110.00	83	0.800
11	17	10	10	4	109.00	86	0.667

3.2 Statistical Analysis — Response Y_1: Particle Size

3.2.1 ANOVA and Model Significance

ANOVA results for the quadratic model fitted to particle size data are presented in Table 4. The model was highly significant ($F = 34.14$, $p < 0.0001$), confirming that the relationship between the tested formulation variables and particle size is not attributable to random noise. Compritol 888 ATO concentration (Factor A) was overwhelmingly dominant, accounting for 603.09/696.50 = 86.6% of the total corrected sum of squares ($F = 272.12$, $p < 0.0001$). This reflects the central role of the lipid matrix: higher Compritol concentrations increase the viscosity of the molten lipid phase, producing larger droplets during high-shear homogenisation that solidify into correspondingly larger nanoparticles. Tween 80 (Factor C) exerted a significant linear effect ($F = 8.12$, $p = 0.0247$), with increasing co-surfactant concentrations marginally increasing PS — likely attributable to competitive adsorption at the lipid-water interface that partially displaces the more effective steric stabiliser Poloxamer 188. The quadratic terms A^2 ($F = 10.04$, $p = 0.0157$) and C^2 ($F = 6.41$, $p = 0.0392$) were also significant, indicating non-linear curvature in the PS response at the extremes of Compritol and Tween 80 ranges.

Table 4. ANOVA for quadratic model — Response Y_1: Particle Size.

Source	SS	df	MS	F-value	p-value	Significance
Model	**680.98**	**9**	**75.66**	**34.14**	**< 0.0001**	★ Significant
A – Compritol 888 ATO	603.09	1	603.09	272.12	< 0.0001	★ Most dominant
B – Poloxamer 188	5.35	1	5.35	2.41	0.1643	Not significant
C – Tween 80	18.00	1	18.00	8.12	0.0247	★ Significant
AB	7.45	1	7.45	3.36	0.1093	Not significant
AC	1.00	1	1.00	0.45	0.5233	Not significant
BC	4.00	1	4.00	1.80	0.2210	Not significant

Source	SS	df	MS	F-value	p-value	Significance
A^2	22.24	1	22.24	10.04	0.0157	★ Significant
B^2	7.10	1	7.10	3.20	0.1166	Not significant
C^2	14.20	1	14.20	6.41	0.0392	★ Significant
Residual	15.51	7	2.22	—	—	
Lack of Fit	12.53	3	4.18	5.61	0.0646	Borderline ($p < 0.10$)
Pure Error	2.98	4	0.75	—	—	
Corrected Total	**696.50**	**16**	—	—	—	

Particle Size Model Equation (Coded Factors):

$$PS = 109.54 + 8.68A - 0.82B + 1.50C - 1.36AB + 0.50AC + 1.00BC + 2.30A^2 + 1.30B^2 - 1.84C^2$$

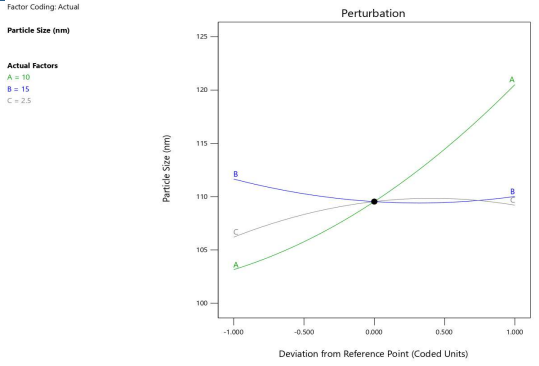

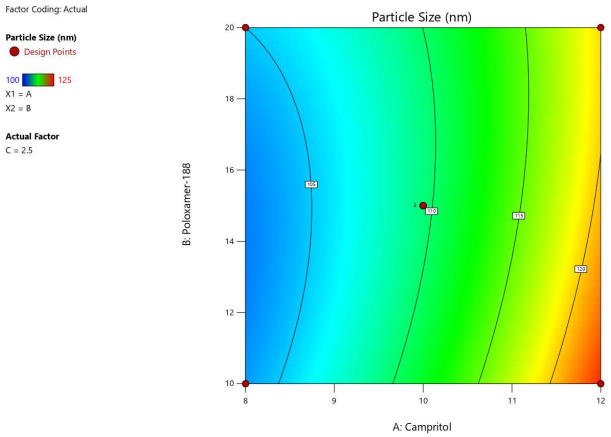

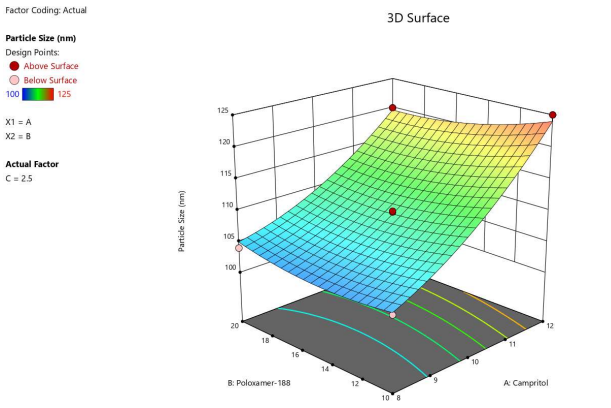

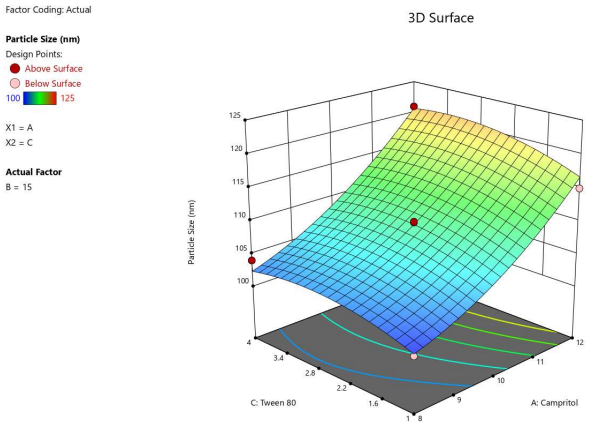

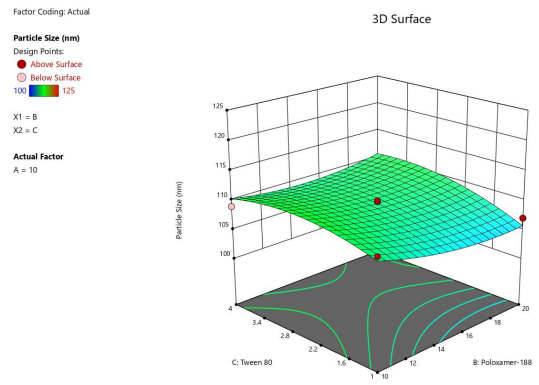

3.3 Statistical Analysis — Response Y_2: Entrapment Efficiency

3.3.1 Model Fit Summary

Model fit summary for EE confirmed that the quadratic model was the most appropriate (sequential p = 0.0031; Lack of Fit p = 0.1985; Adjusted R^2 = 0.8892; Predicted R^2 = 0.4680), clearly superior to the linear (Adjusted R^2 = 0.306) and 2FI (Adjusted R^2 = 0.494) models. The cubic model was aliased (insufficient degrees of freedom) and therefore not considered.

3.3.2 ANOVA Results for EE

The quadratic EE model was significant (F = 15.27, p = 0.0008; Table 5). The significant model terms were: Factor A — Compritol (F = 51.94, p = 0.0002), Factor B — Poloxamer 188 (F = 8.57, p = 0.0221), the AB synergistic interaction (F = 32.87, p = 0.0007), and the B^2 quadratic term (F = 32.70, p = 0.0007). The AB interaction is the most practically important finding: it demonstrates that the effect of Compritol concentration on EE is not independent of Poloxamer 188 concentration. At higher Compritol concentrations (denser lipid matrix), higher Poloxamer 188 concentrations are needed to adequately stabilise the expanded lipid-water interface and prevent drug partitioning into the aqueous phase. The strong B^2 curvature indicates a non-linear optimum of Poloxamer 188 — both insufficient and excessive Poloxamer concentrations reduce EE, the former by inadequate interfacial coverage and the latter by potential micellar solubilisation of the drug. The non-significant Lack of Fit (p = 0.1985) confirms satisfactory model fit.

Table 5. ANOVA for quadratic model — Response Y_2: Entrapment Efficiency.

Source	SS	df	MS	F-value	p-value	Significance
Model	**338.75**	**9**	**37.64**	**15.27**	**0.0008**	★ Significant
A – Compritol 888 ATO	128.00	1	128.00	51.94	0.0002	★ Significant
B – Poloxamer 188	21.13	1	21.13	8.57	0.0221	★ Significant
C – Tween 80	6.13	1	6.13	2.49	0.1589	Not significant
AB	81.00	1	81.00	32.87	0.0007	★ Strong synergy
AC	1.00	1	1.00	0.41	0.5444	Not significant
BC	6.25	1	6.25	2.54	0.1553	Not significant
A^2	1.64	1	1.64	0.67	0.4409	Not significant
B^2	80.59	1	80.59	32.70	0.0007	★ Strong curvature
C^2	7.96	1	7.96	3.23	0.1153	Not significant
Residual	17.25	7	2.46	—	—	
Lack of Fit	11.25	3	3.75	2.50	0.1985	Not significant (good fit)
Pure Error	6.00	4	1.50	—	—	
Corrected Total	**356.00**	**16**	—	—	—	

EE Model Equation (Coded Factors): EE = 83.00 + 4.00A + 1.63B + 0.88C + 4.50AB − 0.50AC + 1.25BC + 0.63A² + 4.37B² + 1.38C²

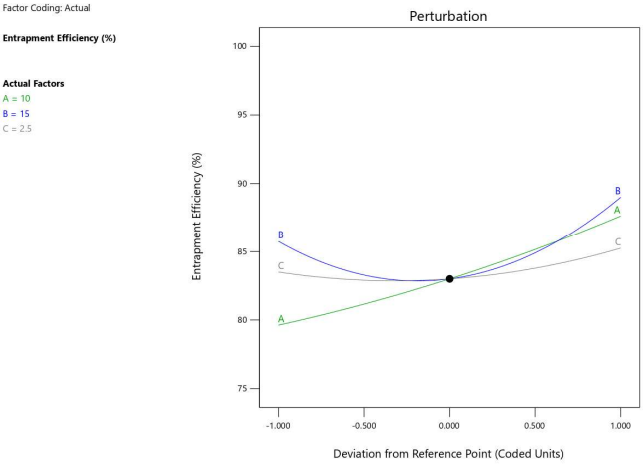

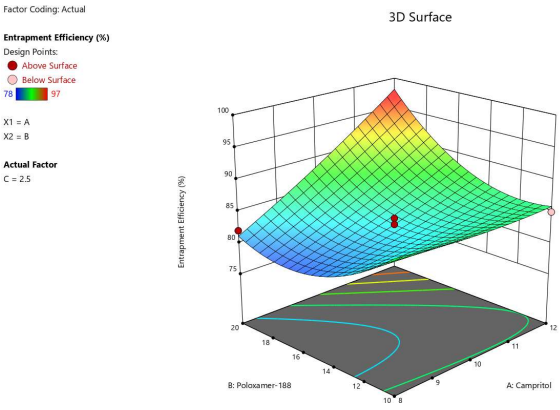

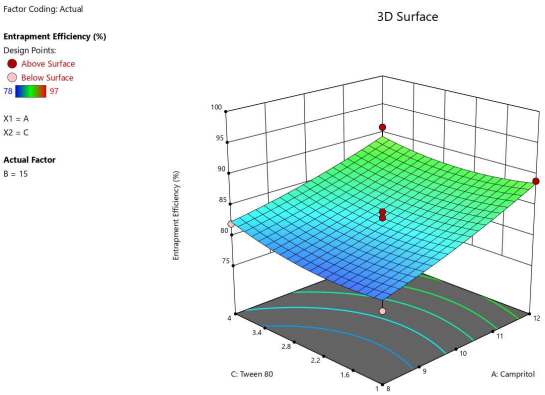

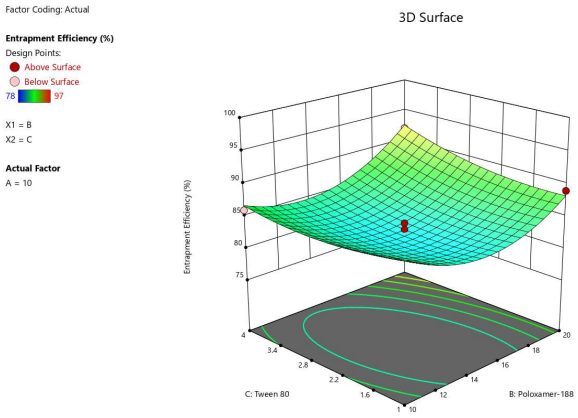

3.4 Statistical Analysis — Response Y₃: Polydispersity Index

The PDI quadratic model was significant (F = 6.10, p = 0.0132; Table 6). Only Factor A linear (F = 36.84, p = 0.0005) and C² quadratic (F = 10.24, p = 0.0151) terms achieved statistical significance. The dominant linear effect of Compritol on PDI mirrors its effect on PS: higher Compritol produces not only larger but also more heterogeneous particles (coefficient = +0.1312 per coded unit). The negative C² coefficient (−0.0954) indicates an inverted-U (concave-down) relationship between Tween 80 and PDI — PDI is highest at both extremes of Tween 80 (1 mL and 4 mL), with a minimum in the intermediate range (~2.5 mL). This reflects surfactant kinetic competition dynamics: insufficient Tween 80 leaves the interface inadequately stabilised, while excess Tween 80 promotes desorption of Poloxamer 188, both resulting in broader particle size distributions. The Lack of Fit was non-significant (p = 0.7552), confirming adequate model fit.

Table 6. ANOVA for quadratic model — Response Y₃: PDI.

Source	SS	df	MS	F-value	p-value	Significance
Model	**0.2052**	**9**	**0.0228**	**6.10**	**0.0132**	★ Significant
A – Compritol 888 ATO	0.1378	1	0.1378	36.84	0.0005	★ Most dominant
B – Poloxamer 188	0.0003	1	0.0003	0.07	0.7937	Not significant

Source	SS	df	MS	F-value	p-value	Significance
C – Tween 80	0.0007	1	0.0007	0.19	0.6777	Not significant
AB	0.0011	1	0.0011	0.28	0.6116	Not significant
AC	0.0007	1	0.0007	0.19	0.6778	Not significant
BC	0.0023	1	0.0023	0.62	0.4583	Not significant
A^2	0.0123	1	0.0123	3.30	0.1121	Not significant
B^2	0.0128	1	0.0128	3.42	0.1070	Not significant
C^2	0.0383	1	0.0383	10.24	0.0151	★ Significant
Residual	0.0262	7	0.0037	—	—	
Lack of Fit	0.0062	3	0.0021	0.41	0.7552	Not significant (good fit)
Pure Error	0.0200	4	0.0050	—	—	
Corrected Total	**0.2314**	**16**	—	—	—	

PDI Model Equation (Coded Factors): $PDI = 0.7228 + 0.1312A + 0.0059B + 0.0094C - 0.0162AB - 0.0132AC + 0.0240BC - 0.0541A^2 + 0.0551B^2 - 0.0954C^2$

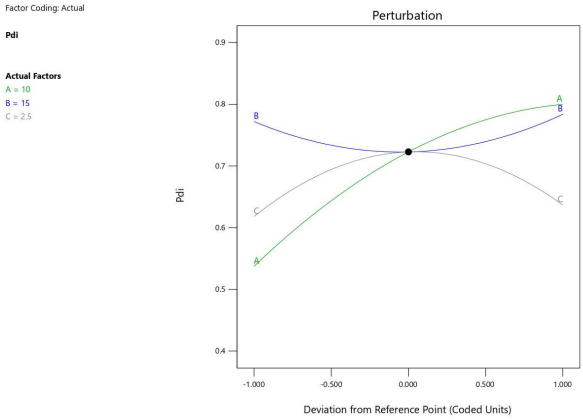

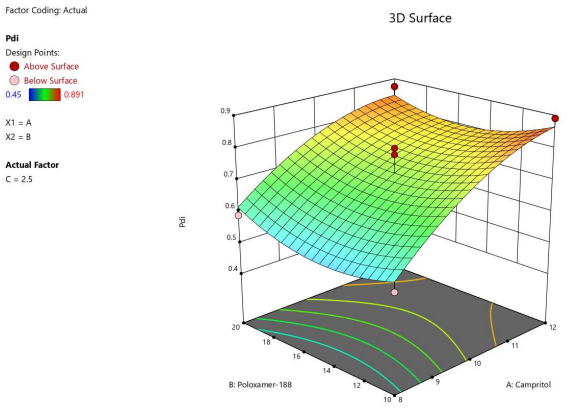

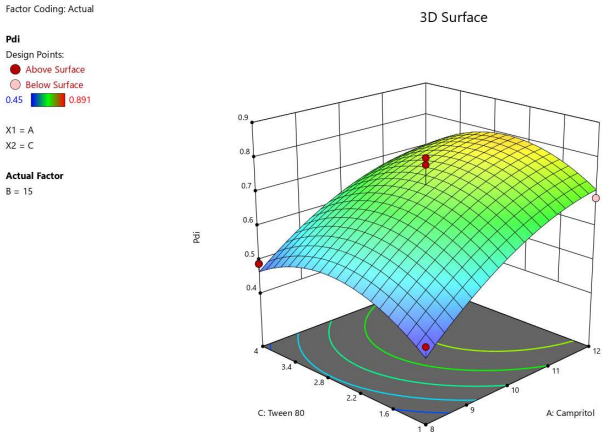

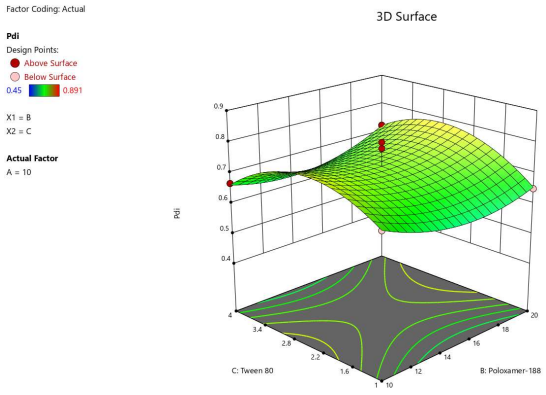

3.5 Comparative Model Fit Statistics

Comparative fit statistics for all three quadratic models are summarised in Table 7. The PS model demonstrated the highest internal fit (R^2 = 0.9777, Adjusted R^2 = 0.9491) and the strongest signal-to-noise ratio (Adequate Precision = 20.74). The EE model showed intermediate fit (R^2 = 0.9515, Adjusted R^2 = 0.8892; Adequate Precision = 15.37). The PDI model had the weakest fit (R^2 = 0.8868, Adjusted R^2 = 0.7414; Adequate Precision = 9.51), consistent with the greater measurement variability inherent to DLS-derived PDI values (CV = 9.02%).

Table 7. Comparative fit statistics for all three quadratic response surface models.

Metric	Y_1: PS	Y_2: EE	Y_3: PDI
R^2	0.9777	0.9515	0.8868
Adjusted R^2	0.9491	0.8892	0.7414
Predicted R^2	0.7054	0.4680	0.4391
Adequate Precision	20.74	15.37	9.51
Std. Dev.	1.49	1.57	0.0612
CV (%)	1.35	1.83	9.02
Mean	110.37 nm	86.00 %	0.6784

The Predicted R^2 values (0.7054, 0.4680, and 0.4391 for PS, EE, and PDI, respectively) differ from their respective Adjusted R^2 values by more than 0.2 for all three responses. This pattern is characteristic of BBD, with a large number of model terms (9) relative to the number of experimental runs (17), resulting in high leverage for individual observations. This diagnostic indicates that while the models are reliable for interpolation within the design space, confirmation runs at the predicted optimum are essential before any optimisation claim can be finalised. All three Adequate Precision ratios exceed the minimum desirable threshold of 4.0, confirming that each model provides an adequate signal for design space navigation.

3.6 Optimised Formulation and Physicochemical Characterisation

3.6.1 Selection of Optimised Formulation

Based on model analysis and the objective of simultaneously minimising particle size, maximising EE, and achieving a PDI in the acceptable range, the following formulation was selected as the optimised combination:

Table 8. Composition of the optimised cilnidipine-loaded SLN formulation.

Ingredient	Quantity
Cilnidipine (Drug)	100.0 mg
Compritol 888 ATO (Glycerol Dibehenate)	10.0 g
Tween 80	2.5 ml
Poloxamer 188	15.0 g
Purified Water	q.s.

3.6.2 Particle Size and Zeta Potential

The optimised cilnidipine SLN formulation exhibited a mean particle size of 121 nm (Figure 1), firmly within the sub-200 nm nanoparticle range considered optimal for colloidal stability and transdermal delivery [20]. This particle size is consistent with the BBD-predicted optimum for the centre-point factor combination. It reflects the balanced stabilisation provided by Poloxamer 188 and Tween 80 at their mid-range concentrations. The zeta potential of the optimised formulation was −41.05 mV (Figure 2), well below the conventional stability threshold of −30 mV. This strongly negative surface charge generates sufficient electrostatic repulsion to prevent aggregation and flocculation [21]. The high zeta potential is attributed to the adsorption of Poloxamer 188's poly (ethylene oxide) (PEO) chains onto the particle surface, resulting in combined electrosteric stabilisation. The low PDI observed for this formulation (0.46) confirms the reasonable size uniformity of the preparation.

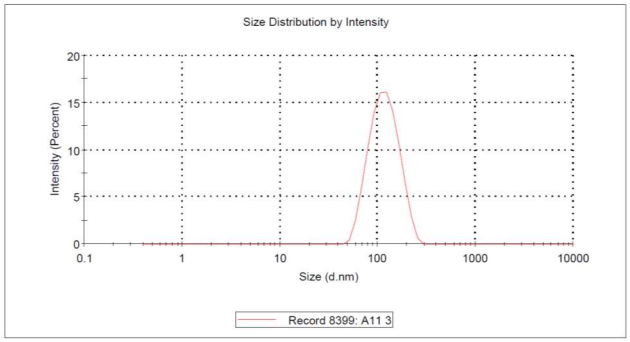

Figure 1: Particle size distribution of Cilnidipine SLN

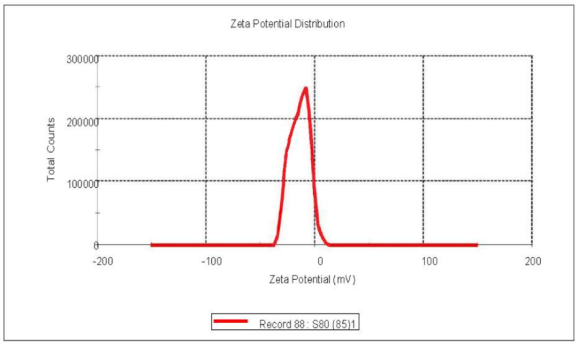

Figure 2: Zeta potential of Cilnidipine SLN

3.6.3 Entrapment Efficiency

The EE of the optimised SLN formulation was 84.34%. This value reflects the strong lipophilic affinity of cilnidipine (log P ~4.7) for the Compritol 888 ATO solid lipid matrix. The relatively high EE confirms that the melt-emulsification method — in which the drug is dissolved in IPA and incorporated into the molten lipid before emulsification — ensures intimate drug-lipid mixing and effective encapsulation within the lipid core before solidification. Minor losses (~15.66%) may be attributable to drug partitioning into the aqueous surfactant phase during homogenisation or to surface-adsorbed drug fractions that are not firmly entrapped within the lipid matrix.

3.6.4 Scanning Electron Microscopy

SEM analysis of the optimised cilnidipine SLN formulation (Figure 3) confirmed the formation of discrete nanoparticles with predominantly spherical-to-oval morphology, consistent with the expected geometry of SLNs produced by melt emulsification [22]. Mild agglomeration was observed in the dried SEM specimens — a common artefact of the drying step during specimen preparation that does not reflect the dispersion state of the SLNs in the liquid medium, as confirmed by DLS. Particle surfaces appeared relatively smooth, with no visible drug crystals projecting from the lipid matrix surface — indicating uniform drug encapsulation within the lipid core rather than surface deposition. The particle dimensions observed by SEM were consistent with the DLS-derived size measurements (122 nm), providing orthogonal confirmation of the nanoparticle size range.

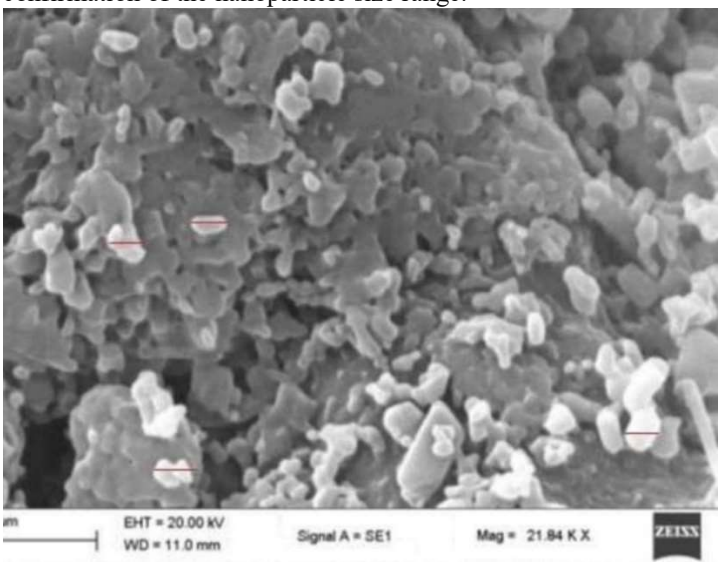

Figure 3: SEM image of Cilnidipine SLN

3.7 In Vitro Drug Release Studies

The cumulative in vitro drug-release profile of the optimised cilnidipine SLNs over 24 hours in PBS (pH 7.4, 37°C) is presented in Table 8 and illustrated in Figure 4. A characteristic biphasic drug-release pattern was observed throughout the study.

The initial burst release phase was evident within the first hour, during which approximately 30.68 ± 0.48% of cilnidipine was released. This rapid initial phase is attributed to the rapid dissolution of drug molecules adsorbed on or near the outer lipid shell surface, which are readily accessible to the PBS release medium without requiring diffusion through the lipid core [23]. The ~30% burst release is clinically advantageous for an antihypertensive indication, providing a rapid onset of pharmacological effect.

Following the initial burst, a gradual, controlled release phase was observed from 1 to 24 hours: cumulative release reached 39.52 ± 0.42% at 2 h; 53.35 ± 0.46% at 4 h; 65.96 ± 0.40% at 6 h; 74.25 ± 0.51% at 8 h; 80.84 ± 0.58% at 12 h; and 83.46 ± 0.52% at 24 h. The sustained-release phase reflects diffusion-controlled transport of cilnidipine through the crystalline or amorphous lipid matrix, a well-established mechanism of SLN-mediated drug delivery [24]. The tortuous lipid lattice substantially retards drug diffusion, resulting in the observed prolonged release profile.

This biphasic release pattern — characterised by a manageable initial burst followed by sustained release over 24 h — is well-suited to the pharmacotherapeutic requirements of hypertension management, where rapid onset of action combined with prolonged therapeutic drug concentrations is clinically advantageous [25, 26]. The release behaviour further supports the potential of this formulation for transdermal drug delivery, where

controlled permeation over extended periods is essential for maintaining steady plasma drug levels.

Table 8. In vitro cumulative drug release profile of optimised cilnidipine-loaded SLNs (dialysis membrane method, PBS pH 7.4, 37°C, n = 3, mean ± SD).

S. No.	Time (h)	Cumulative Drug Release (%, mean ± SD)
1	0	0 ± 0.00
2	0.25	7.22 ± 0.39
3	0.50	13.58 ± 0.42
4	0.75	22.16 ± 0.37
5	1.00	30.68 ± 0.48
6	2.00	39.52 ± 0.42
7	4.00	53.35 ± 0.46
8	6.00	65.96 ± 0.40
9	8.00	74.25 ± 0.51
10	10.00	78.66 ± 0.38
11	12.00	80.84 ± 0.58
12	24.00	83.46 ± 0.52

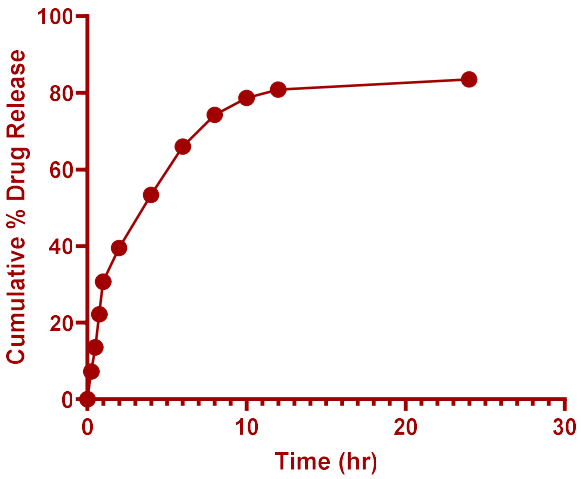

Figure 4: In vitro drug release profile of the optimised cilnidipine-loaded SLN

4. CONCLUSION

The present study successfully demonstrated the application of a Box-Behnken design-driven response surface methodology to systematically optimise cilnidipine-loaded solid lipid nanoparticles. The three-factor, three-level BBD efficiently mapped the influence of Compritol 888 ATO, Poloxamer 188, and Tween 80 on three CQAs across 17 experimental runs. Statistical analysis identified quadratic models as significant for all three responses. Compritol 888 ATO concentration was the dominant factor governing particle size (F = 272.12) and PDI (F = 36.84). At the same time, a critical synergistic interaction between Compritol and Poloxamer 188 was identified as the primary determinant of entrapment efficiency (F = 32.87). Adequate Precision values exceeding 9.5 for all responses confirmed the navigability of the established design space.

The optimised SLN formulation was prepared by melt-emulsification/high-shear homogenisation and characterised comprehensively: particle size of 122 nm, zeta potential of −41.05 mV (indicating excellent colloidal stability), EE of 84.34%, and spherical-to-oval morphology by SEM. In vitro drug release demonstrated a clinically advantageous biphasic profile — a rapid-onset burst (~30.68% in 1 h) followed by sustained release reaching 83.46% over 24 hours — consistent with the controlled-release pharmacokinetics desirable for a once-daily antihypertensive agent. Franz diffusion cell studies further supported the formulation's transdermal applicability.

Collectively, these findings establish that Box-Behnken-optimised SLNs represent a robust and scalable platform for cilnidipine delivery, with the potential to overcome its BCS Class II biopharmaceutical limitations and enable controlled transdermal application. Future work should include in vivo pharmacokinetic evaluation in appropriate animal models, ex vivo skin permeation studies using excised human or rat skin, stability studies under ICH conditions, and confirmation runs at the predicted optimum to validate the model predictions fully.

DECLARATIONS

Authors' Contributions:

Nishant Yadav: Conceptualisation, laboratory experiments, data collection, characterisation.
Sushma Devi: Manuscript writing.
Teenu Sharma: Study design and statistical analysis.
Parveen Kumar: Manuscript writing and statistical analysis

Acknowledgements:

The authors gratefully thank Pure & Cure Healthcare Pvt. Ltd., Haridwar, India, for the gift sample of cilnidipine.

REFERENCES

[1] WHO. Global Report on Hypertension: The Race Against a Silent Killer. Geneva: World Health Organisation; 2023.

[2] Mancia G, Kreutz R, Brunström M, et al. 2023 ESH Guidelines for the management of arterial hypertension. J Hypertens. 2023;41(12):1874–2071.

[3] Yadav N, Kumar P, Singh TG, Devi S. Nanotechnology-Enhanced Transdermal Patches for Hypertension: A Review. Current Hypertension Reviews. 2025 Apr 28.

[4] Kai T, Kuzumoto Y. Effects of a dual L/N-type calcium channel blocker cilnidipine on blood pressure, pulse rate, and autonomic functions in patients with mild to moderate hypertension. Clinical and Experimental Hypertension. 2009 Nov 1;31(7):595-604.

[5] Lee J, Lee H, Jang K, Lim KS, Shin D, Yu KS. Evaluation of the pharmacokinetic and pharmacodynamic drug interactions between cilnidipine and valsartan, in healthy volunteers. Drug design, development and therapy. 2014 Oct 8:1781-8.

[6] ICH Harmonised Guideline. Biopharmaceutics Classification System-Based Biowaivers M9. International Council for Harmonisation; 2019.

[7] Müller RH, Mäder K, Gohla S. Solid lipid nanoparticles (SLN) for controlled drug delivery — a review of the state of the art. Eur J Pharm Biopharm. 2000;50(1):161–177.

[8] Mehnert W, Mäder K. Solid lipid nanoparticles: production, characterisation and applications. Adv Drug Deliv Rev. 2001;47(2–3):165–196.

[9] Severino P, Andreani T, Macedo AS, et al. Current state-of-art and new trends on lipid nanoparticles for oral drug delivery. J Drug Deliv. 2012;2012:750891.

[10] Pardeike J, Hommoss A, Müller RH. Lipid nanoparticles (SLN, NLC) in cosmetic and pharmaceutical dermal products. Int J Pharm. 2009;366(1–2):170–184.

[11] Montgomery DC. Design and Analysis of Experiments. 10th ed. Hoboken, NJ: Wiley; 2020.

[12] Box GEP, Behnken DW. Some new three-level designs for the study of quantitative variables. Technometrics. 1960;2(4):455–475.

[13] Clogston JD, Patri AK. Zeta potential measurement. InCharacterization of nanoparticles intended for drug delivery 2010 Oct 19 (pp. 63-70). Totowa, NJ: Humana press.

[14] Souto EB, Wissing SA, Barbosa CM, Müller RH. Evaluation of the physical stability of SLN and NLC before and after incorporation into hydrogel formulations. Eur J Pharm Biopharm. 2004;58(1):83–90.

[15] Bhalekar MR, Pokharkar V, Madgulkar A, Patil N. Preparation and evaluation of miconazole nitrate-loaded solid lipid nanoparticles for topical delivery. AAPS PharmSciTech. 2009;10(1):289–296.

[16] Goldstein JI, Newbury DE, Michael JR, et al. Scanning Electron Microscopy and X-Ray Microanalysis. 4th ed. New York: Springer; 2018.

[17] Blanco E, Shen H, Ferrari M. Principles of nanoparticle design for overcoming biological barriers to drug delivery. Nature biotechnology. 2015 Sep;33(9):941-51.

[18] Kipriye Z, Şenel B, Yenilmez E. Preparation and evaluation of carvedilol-loaded solid lipid nanoparticles for targeted drug delivery. Tropical journal of pharmaceutical research. 2017 Sep 1;16(9).

[19] Paudel KS, Milewski M, Swadley CL, Brogden NK, Ghosh P, Stinchcomb AL. Challenges and opportunities in dermal/transdermal delivery. Therapeutic delivery. 2010 Jul 1;1(1):109-31.

[20] Wissing SA, Kayser O, Müller RH. Solid lipid nanoparticles for parenteral drug delivery. Adv Drug Deliv Rev. 2004;56(9):1257–1272.

[21] Riddick TM. Control of Colloid Stability Through Zeta Potential. Wynnewood, PA: Livingston Publishing; 1968.

[22] Zhang L, Gu FX, Chan JM, et al. Nanoparticles in medicine: therapeutic applications and developments. Clin Pharmacol Ther. 2008;83(5):761–769.

[23] Viegas C, Patrício AB, Prata JM, Nadhman A, Chintamaneni PK, Fonte P. Solid Lipid Nanoparticles vs. Nanostructured Lipid Carriers: A Comparative Review. Pharmaceutics. 2023 May 25;15(6):1593. doi: 10.3390/pharmaceutics15061593. PMID: 37376042; PMCID: PMC10305282.

[24] Freitas C, Müller RH. Effect of light and temperature on zeta potential and physical stability in SLN dispersions. Int J Pharm. 1998;168(2):221–229.

[25] Müller RH, Rühl D, Runge S, et al. Cytotoxicity of solid lipid nanoparticles as a function of the lipid matrix and the surfactant. Pharm Res. 1997;14(4):458–462.

[26] Mishra V, Bansal KK, Verma A, et al. Solid lipid nanoparticles: emerging colloidal nano drug delivery systems. Pharmaceutics. 2018;10(4):191.